PAR-3 is required for epithelial cell polarity in the distal spermatheca of *C. elegans*

Shinya Aono[1,*], Renaud Legouis[2], Wendy A. Hoose[1] and Kenneth J. Kemphues[1,†]

[1]Department of Molecular Biology and Genetics, Cornell University, 107 Biotechnology Building, Ithaca, NY 14853, USA
[2]CNRS-CGM, Avenue de la Terasse, 91198 Gif-sur-Yvette, France
*Present address: Department of Molecular Biology, Yokohama City University School of Medicine, 3-9 Fuku-ura, Kanazawa-Ku, Yokohama 236-0004, Japan
†Author for correspondence (e-mail: kjk1@cornell.edu)

Accepted 26 February 2004

Development 131, 2865-2874
Published by The Company of Biologists 2004
doi:10.1242/dev.01146

Summary

PAR-3 is localized asymmetrically in epithelial cells in a variety of animals from *Caenorhabditis elegans* to mammals. Although *C. elegans* PAR-3 is known to act in early blastomeres to polarize the embryo, a role for PAR-3 in epithelial cells of *C. elegans* has not been established. Using RNA interference to deplete PAR-3 in developing larvae, we discovered a requirement for PAR-3 in spermathecal development. Spermathecal precursor cells are born during larval development and differentiate into an epithelium that forms a tube for the storage of sperm. Eggs must enter the spermatheca to complete ovulation. PAR-3-depleted worms exhibit defects in ovulation. Consistent with this phenotype, PAR-3 is transiently expressed and localized asymmetrically in the developing somatic gonad, including the spermathecal precursor cells of L4 larvae. We found that the defect in ovulation can be partially suppressed by a mutation in IPP-5, an inositol polyphosphate 5-phosphatase, indicating that one effect of PAR-3 depletion is disruption of signaling between oocyte and spermatheca. Microscopy revealed that the distribution of AJM-1, an apical junction marker, and apical microfilaments are severely affected in the distal spermatheca of PAR-3-depleted worms. We propose that PAR-3 activity is required for the proper polarization of spermathecal cells and that defective ovulation results from defective distal spermathecal development.

Key words: Cell polarity, Ovulation, Gonadogenesis, *Caenorhabditis elegans*

Introduction

Acquisition of cell polarity is important to epithelial cells for carrying out their barrier function and for their proper movements during morphogenesis (Knust and Bossinger, 2002; Ohno, 2001). The formation of zonula adherens is a key step in epithelial polarization. Zonula adherens are belt-like cell-cell junctions at the apex of polarized epithelial cells and are called apical junctions in *Caenorhabditis elegans*. From genetic studies on *Drosophila* embryonic ectoderm, *C. elegans* gut epithelium and mammalian culture cells, it appears that three independent protein-complexes accumulating along the plasma membrane are required for regulating the formation of this specialized junctional structure: the PAR-3/PAR-6/aPKC complex, the Scribble/Dlg/Lgl complex, and the Crumbs/Stardust complex (Betschinger et al., 2003; Bilder et al., 2003; Hurd et al., 2003; Johnson and Wodarz, 2003; Knust and Bossinger, 2002; Plant et al., 2003; Tanentzapf and Tepass, 2003; Yamanaka et al., 2003).

One of these complexes, the PAR-3/PAR-6/aPKC complex, plays a fundamental role in establishing cell polarities essential for asymmetric divisions in the early embryo in *C. elegans* (for reviews, see Kemphues and Strome, 1997; Pellettieri and Seydoux, 2002), but to date there has been no evidence for a role in epithelial polarity in this animal. Based on the conservation of the biochemical interactions between PAR-3 and PAR-6 family members and their conserved role in epithelial polarity in flies and mammals (Izumi et al., 1998; Johnson and Wodarz, 2003; Knust and Bossinger, 2002; Kuchinke et al., 1998; Ohno, 2001), it seems reasonable to expect a role for the complex in epithelial polarity in *C. elegans* as well. The proteins are expressed and co-localized apically in *C. elegans* gut and vulva (Hurd and Kemphues, 2003; Leung et al., 1999; McMahon et al., 2001), consistent with a role in one or both of these polarized epithelia. However, none of the existing mutants in *par-3* and *par*-6, including amber mutations in *par-3* (Cheng et al., 1995; Watts et al., 1996), results in obvious defects in polarized epithelia. It is possible that roles in epithelial development are masked by persistence of wild-type maternal mRNA and protein in homozygous progeny derived from heterozygous mothers and by the polarity defect in early embryos produced by homozygous mutant mothers. Indeed, it has recently been shown that PAR-3 has a role in cell adhesion and gastrulation in the early embryo that is only revealed when the early polarity requirement is bypassed (Nance et al., 2003). To explore a possible role for PAR-3 in vulval development, we depleted PAR-3 post-embryonically using RNAi.

Unexpectedly, we found that PAR-3-depleted worms exhibit defects in ovulation and fail to store sperm properly due to defective functioning of the spermatheca. The spermatheca is a tubular epithelium that acts in sperm storage, ovulation and fertilization. We discovered that PAR-3 is transiently expressed

and localized asymmetrically at or near apical junctions in spermathecal precursor cells of L4 larvae. We also found that the cell polarity of a subset of cells in the distal spermatheca is severely affected in PAR-3 depleted worms. Finally, we determined that the ovulation defects of *par-3(RNAi)* worms can be suppressed by a mutation that can bypass defects in signaling between the oocyte and the spermatheca. From these observations, we propose that PAR-3 activity is necessary for the proper polarization of cells in the distal spermatheca and that defective ovulation and storage of mature sperm result from failure of the distal spermathecal cells to respond to signals from the oocyte that trigger spermathecal dilation.

Materials and methods

Nematode culture and strains

Nematodes for these experiments were grown according to standard procedures, but at 25°C rather than 20°C to optimize the effects of RNAi feeding. Because growth at 25°C is more rapid than at lower temperatures, the times of key developmental events are earlier than other published studies. For example, at 25°C, the L3-L4 molt occurs at 30-31 hours after hatching and the L4-adult molt occurs at 39-41 hours after hatching. Semi-synchronized L1s were obtained by hatching and starvation in M9 salts (Lewis and Fleming, 1995). Strain SU93, AJM-1::GFP translational fusion (AJM-1 was formerly JAM-1) (Michaux et al., 2001; Mohler et al., 1998), and PS3653 *ipp-5*(*sy605*) (Bui and Sternberg, 2002) were obtained from the Caenorhabditis Genetics Center stock collection (University of Minnesota, St Paul, MN). Strain ML625, LET-413::GFP (Legouis et al., 2000) and the strain JJ1136, HMP-1::GFP (Raich et al., 1999) translation fusion strains were acquired from M. Labouesse and J. Hardin, respectively. Strain HR606, the *let-502::gfp* promoter fusion (Wissmann et al., 1999), and strain PD8488 *rrf-1*(*pk1417*) (Sijen et al., 2001) were kindly provided by P. Mains, and T. Schedl respectively. Strain PS3747, IPP-5::GFP translational fusion (Bui and Sternberg, 2002), was obtained from P. Sternberg. Strain GE2623, *par-3(t1591) unc-32(e189) / qC1* was isolated and provided by R. Schnabel.

RNAi

In initial experiments, we tested independently the NH_2-terminal 1.6 kb fragment of *par-3* (GenBank Accession Number U25032) (nucleotides 1-1686 (X1)) and three internal fragments obtained by restriction digest of *Hin*dIII (nucleotides 840-1888 (H1), 1889-2755 (H2) and 2756-4277 (H3)). Throughout this study, we used the NH_2-terminal construct as it caused the most consistent, highly penetrant Emo phenotype. For RNAi of *par-6* (GenBank Accession Number AF070968) and *pkc-3* (GenBank Accession Number AF025666), we used full-length cDNA clones. Each DNA was inserted into the vector pPD129.36 (Timmons et al., 2001) for expression of *par-3* dsRNA in *Escherichia coli* strain HT115(DE3). Induction and feeding were performed as previously described (Timmons et al., 2001), except that 0.5 mM IPTG was used. HT115(DE3) harboring the empty vector served as control bacteria for the feeding experiments.

Fixation, immunocytochemistry and microscopy

Larvae were fixed in methanol according to standard protocols (Miller and Shakes, 1995). To permeabilize prior to fixation, larvae were compressed between two poly-lysine-coated slides and frozen over dry ice. The slides were rapidly separated, tearing the cuticle in the process, and then immediately immersed in –20°C methanol while still frozen. For staining with DAPI, collected worms were fixed without freezing in 2% paraformaldehyde in phosphate buffered saline (PBS) for 24 hours at 4°C followed by incubation with 1 ug/ml DAPI in TBS (150 mM NaCl, 50 mM Tris-HCl, pH 7.5) for 48 hours at room temperature, and then were mounted on slides for observation. Gonad dissecting and phalloidin staining were performed as described previously (McCarter et al., 1997; Strome, 1986). The protocols in Rose et al. (Rose et al., 1997) were applied for the observation of ovulation in vivo and for staining with anti-myosin antibodies.

Two antibodies to PAR-3 produced identical staining patterns in the somatic gonad precursor cells of developing larvae. These included a previously described antiserum raised against the middle portion of PAR-3 (Etemad-Moghadam et al., 1995) and a monoclonal antibody raised against the same fragment used for the antiserum (Nance et al., 2003). All pictures shown here were obtained with the monoclonal antibody at a dilution of 1:50. Affinity-purified rabbit polyclonal antibody to PAR-6 (Hung and Kemphues, 1999) and affinity-purified rat polyclonal antibody to PKC-3 (Hung and Kemphues, 1999) were used at a 1:20 dilution. A new polyclonal antibody to LET-413 was generated against the central part of the protein (residues 469 to 576) and used at a dilution of 1:5000. The monoclonal antibody to myosin heavy chain A (Miller et al., 1986) and rabbit polyclonal antibody to CEH-18 (Greenstein et al., 1994) were used at 1:50 and 1:200, respectively. Secondary antibodies (Jackson Immunoresearch) were used at 1:400 (for anti-LET-413) or 1:100 (all others).

Differential interference contrast epifluorescence microscopy and digital image capture were performed using an Olympus BX60 fitted with a Hamamatsu Orca C4742-95 camera. Confocal laser scanning microscopy was performed on a Leica TCSSP2. Final figures were assembled using Photoshop (Adobe Systems).

Results

Post-embryonic depletion of PAR-3 results in an Emo phenotype

To understand the role of PAR-3 protein during post-embryonic development, we performed *par-3* RNAi to deplete the protein in developing larvae. Following a previous study in our laboratory (Hurd and Kemphues, 2003), we placed synchronized L1 larvae on plates with bacteria expressing double strand RNA transcribed from the first 1.6 kb portion of *par-3* cDNA (see Materials and methods). In these slightly asynchronous cultures, by 39 hours after initiating feeding at 25°C, most of the worms have reached adulthood.

A comparison of *par-3(RNAi)* and control worms revealed a slightly reduced growth rate in the treated individuals. On average, the treated worms molted into adults 2-3 hours later than controls. This difference is within the range of the developmental variation within each culture. The RNAi-treated worms were as motile as wild-type worms, suggesting that the neuromuscular system developed normally. However, the reproductive system seemed to be damaged severely, as few eggs were laid by *par-3(RNAi)* worms. As this phenotype had not been reported previously after analysis of *par-3* mutant worms (Cheng et al., 1995), we decided to examine this further. First, we compared the number of embryos present on plates containing 10 control versus 10 RNAi worms after 48 hours of growth. The control plate had >500 embryos, whereas the *par-3(RNAi)* plate had only 70. These results suggest that PAR-3 depletion affects oogenesis or ovulation. Supporting this hypothesis, the most proximal part of the ovary was distended (data not shown). To investigate the phenotype further, we visualized the DNA in oocytes by staining with DAPI and noted that these worms showed an endomitotic oocyte (Emo) phenotype (n>50) (Fig. 1B) (Iwasaki et al., 1996). This phenotype commonly arises through defects in ovulation.

During normal oogenesis, the cell cycle arrests at meiotic

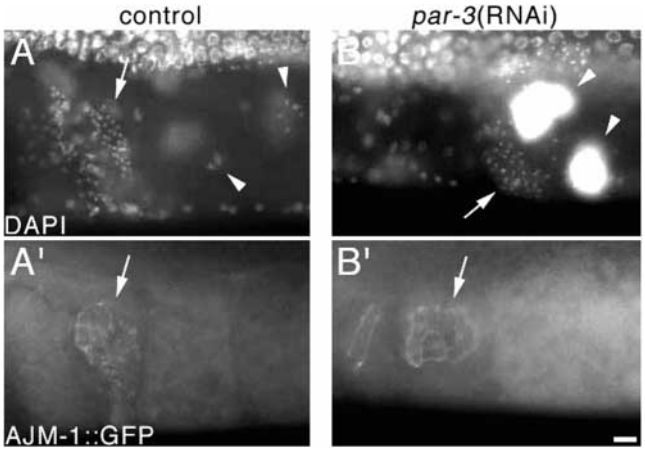

Fig. 1. Post-embryonic phenotype of *par-3(RNAi)* worms. Worms carrying AJM-1::GFP were collected after 48 hours of growth on bacteria producing *par-3* dsRNA (B,B′) or control bacteria (A,A′) and stained with DAPI (A,B). Spermathecae were visualized by AJM-1::GFP (arrows in A′,B′). The small condensed DNA signals represent the sperm nuclei (arrows in A,B) that are present in the spermathecae of control worms (A) but are restricted to the proximal ovary of *par-3(RNAi)* worms (B). Endomitotic oocyte nuclei (B) and normal nuclei (A) are indicated by arrowheads in A, B. Scale bar: 10 μm.

prophase I. Under the influence of signaling from spermatids or spermatozoa and sheath cells, developing oocytes undergo maturation at regular intervals (McCarter et al., 1997, 1999; Miller et al., 2001; Miller et al., 2003). Maturation, marked by the breakdown of the nuclear envelope (NEBD), stimulates contractions of the ovarian sheath that pull the dilating spermatheca over the egg in the process of ovulation (McCarter et al., 1999; Rose et al., 1997). The eggs are fertilized as they enter the spermatheca (Ward and Carrel, 1979). If ovulation fails, the eggs remain unfertilized and undergo endomitotic replication (Greenstein et al., 1994; Iwasaki et al., 1996; McCarter et al., 1997; Rose et al., 1997). Failed ovulation can arise through defects in signaling between oocyte and sheath cells that stimulate contractions (McCarter et al., 1999), through defects in sheath cell differentiation (Greenstein et al., 1994; Rose et al., 1997) or through defects in signaling between the oocyte and the spermatheca (Clandinin et al., 1998).

In addition to the Emo phenotype, we noted that *par-3(RNAi)* worms failed to accumulate sperm in the spermatheca; instead sperm accumulated at the extreme proximal portion of the ovary (n>50 worms) (Fig. 1B). In normal hermaphrodites, sperm are born at the proximal end of the ovotestis during L4 and become localized to the spermatheca by migration or are swept in during the first ovulation (Ward and Carrel, 1979).

These phenotypes are the result of PAR-3 depletion. RNAi using different non-overlapping fragments of *par-3* cDNA gave similar results (43/47 with fragment X1, 37/97 with H1, 31/93 with H2 and 77/103 with H3 showed an Emo phenotype; see Materials and methods). Furthermore, as we describe in detail below, PAR-3 protein was expressed in gonadal cells during their development and was depleted by RNAi.

par-3(RNAi) worms show defects in ovulation

To determine the basis for the Emo phenotype, we examined

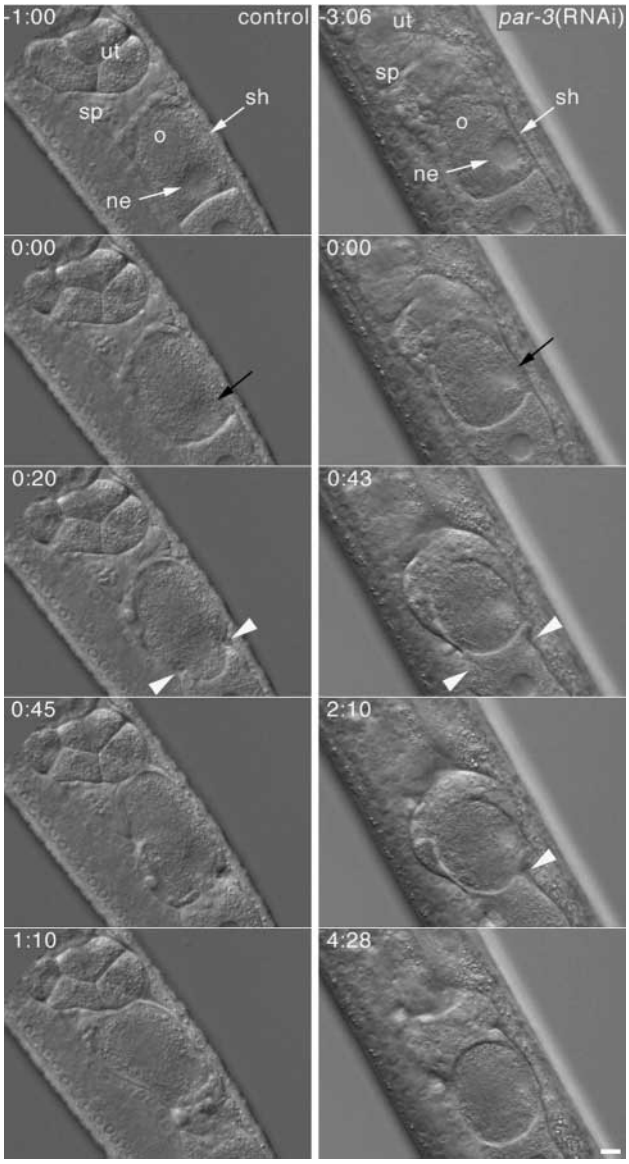

Fig. 2. Defective ovulation in *par-3(RNAi)* worms. Images from time-lapse Nomarski video microscopic observations of meiotic maturation and ovulation in the wild type (left) and a first ovulation in *par-3(RNAi)* (right). Real time (minutes:seconds) is indicated in the top left corner, with the zero time point corresponding to the time that nuclear envelope break down (NEBD) was observed (black arrows). An oocyte (o), the oocyte nuclear envelope (ne), the sheath (sh) and the spermatheca (sp) are indicated. The oocyte enters the spermatheca in the wild type at 0:45 and is transferred to the uterus at 1:10. However, in *par-3(RNAi)* worms, the oocyte remains in the proximal gonad even 4:28 after the NEBD. The contraction of sheath cells and distal extension of the spermatheca was observed in both worms (arrowheads). Scale bar: 10 μm.

oocyte maturation and ovulation in *par-3(RNAi)* worms. During normal ovulation, oocyte maturation, marked by NEBD, is followed by intensive contraction of sheath cells. Oocytes enter the spermatheca within 2 minutes of NEBD (n=5) (Fig. 2, left column). In RNAi-treated worms, NEBD and contraction of sheath cells occurred as in controls, but oocytes had not entered the spermatheca even 4 minutes after NEBD (n=4) (Fig. 2, right

column). Failure to ovulate in spite of vigorous sheath contractions, combined with the observation of mislocalized sperm in adult worms, suggests that the spermatheca, rather than gonad sheath, is not functional in *par-3(RNAi)* worms.

Failure to ovulate could arise due to defects in the oocyte or to defects in the somatic gonad. To distinguish which tissue was being affected by *par-3* RNAi, based on a suggestion by T. Schedl, we used a mutation in the *rrf-1* gene, a putative RNA-dependent RNA polymerase that is required for RNAi in the soma but not in the germline (Sijen et al., 2001). For the experiment, we assayed the frequency of the Emo phenotype and the degree of maternal effect embryonic lethality in control and *rrf-1* worms grown from L1 on bacteria producing *par-3* dsRNA. In three replicates with >70 worms/culture, *par-3* RNAi in the *rrf-1* strain was less effective in producing an Emo phenotype than in the control (10 versus 83%; 32 versus 95%; 25 versus 98%). By contrast, *par-3* RNAi was effective in the germline, because the non-Emo *rrf-1* worms showed a strong maternal effect lethality. Thus, at least a component of the Emo defect is mediated by depletion of PAR-3 in the soma.

Gonad sheath cells develop normally in *par-3(RNAi)* worms

Vigorous sheath cell contractions suggested that the gonad sheath cells were functioning normally after *par-3* RNAi. As a second assay for sheath cell development, we analyzed the expression of sheath-cell-specific markers. Each gonad sheath consists of five pairs of cells arranged in a reproducible pattern and expressing the transcription factor *ceh-18* in the nucleus and myosin heavy chain A (MHCA) in an organized cytoplasmic array (Greenstein et al., 1994; Rose et al., 1997). We compared the distribution of CEH-18 and MHCA in wild-type and *par-3(RNAi)* gonads dissected from worms grown for 48 hours from L1 (young adults). We detected no difference from wild type in the number of sheath cells or in the expression or distribution of the sheath cell markers (for CEH-18, *n*=12 control and *n*=16 *par-3(RNAi)* worms) (Fig. 3A,B) (for MHCA, *n*=50 *par-3(RNAi)* worms) (Fig. 3C,D).

These results suggest that differentiation of gonad sheath is not affected in *par-3(RNAi)* worms. Therefore we focused further analysis on the spermatheca.

Spermathecal cell numbers and cell fates are not affected in *par-3(RNAi)* worms

During early embryogenesis, PAR-3 contributes to asymmetric cell division and cell fate specification. Therefore, we considered the possibility that *par-3* RNAi affected asymmetric division and cell fate specification in the cell lineage leading to the spermatheca. To address the question of whether asymmetric cell divisions were normal, we counted the number of cells in the entire spermatheca after staining nuclear DNA by 0.01 mg/ml of propidium iodide. If the cell division pattern was disorganized, the number of cells in developed tissue could be different from the wild type. However, all nine spermatheca examined contained the expected 30 cells (Kimble and Hirsh, 1979).

To test for proper cell fate specification, we observed the expression of two markers of spermathecal differentiation: GFP fused with the promoters of *let-502*, the homolog of rho-associated kinase (Wissmann et al., 1999) and *ipp-5*, inositol 5-phosphatase (Bui and Sternberg, 2002). The *let-502*-driven

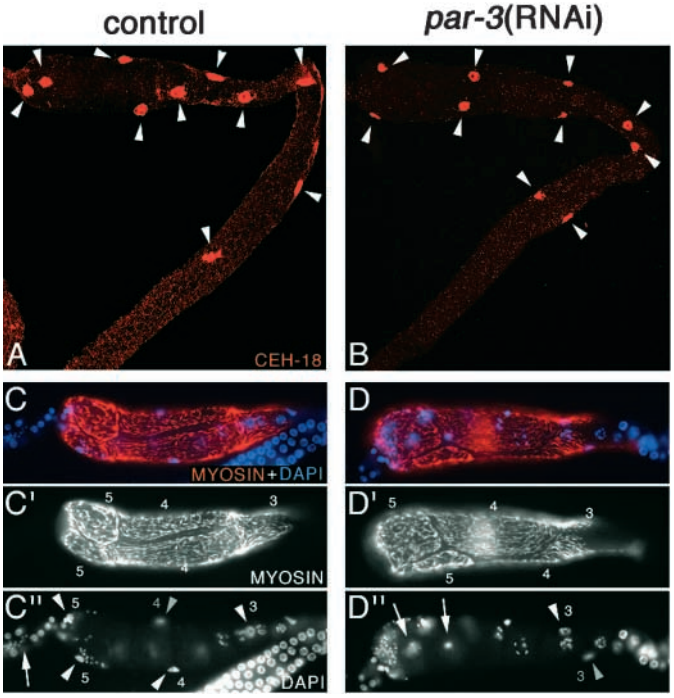

Fig. 3. Differentiation of gonad sheath cells is not affected by *par-3(RNAi)*. (A,B) Expression of CEH-18 protein. Gonads were dissected 48 hours after growth with (right) or without (left) *par-3* RNAi treatment, and stained with anti CEH-18 antibodies. Sheath nuclei are indicated by arrowheads. The size difference in the sheath nuclei in the gonads shown was not reproducible and might have been an artifact of fixation. (C,D) Distribution of myosin heavy chain A (MHCA) in gonad sheath cells of *par-3(RNAi)* worms. Worms were collected after 48 hours of growth with (right) or without (left) RNAi treatment and localization of MHCA was analyzed by epifluorescence microscopy. DNA was stained by DAPI. Sheath cells are numbered and sheath nuclei are indicated by numbered arrowheads; gray arrowheads indicate out of focus nuclei. Scale bar: 10 μm.

GFP protein is expressed in all 30 spermathecal cells, but the level of expression is not even, with highest levels in the proximal and distal cells (Wissmann et al., 1999). In particular, GFP accumulates to extremely high levels in the four distal-most cells (Fig. 4). The *ipp-5*-driven GFP is expressed in the distal region of the adult spermatheca (Bui and Sternberg, 2002). We saw no difference between control and *par-3*(RNAi) worms in the expression of these markers (*n*=21 control and *par-3(RNAi)* worms for *let-502::GFP* and *n*=27 control and *par-3(RNAi)* worms for *ipp-5::GFP*). These results indicate that the specification of cell type or cell division pattern seems not to be disturbed by *par-3(RNAi)*.

However, the organization of the distal cells, as visualized by *let-502::GFP*, was abnormal. Comparing the positions of the cells in treated versus control spermatheca revealed a consistent mis-positioning of the cells and a more variable cell shape (Fig. 4C,D,E).

Ovulation in *par-3(RNAi)* worms is restored by mutation in *ipp-5*, an inositol polyphosphate 5-phosphatase

Defective signaling between oocyte and spermatheca can lead

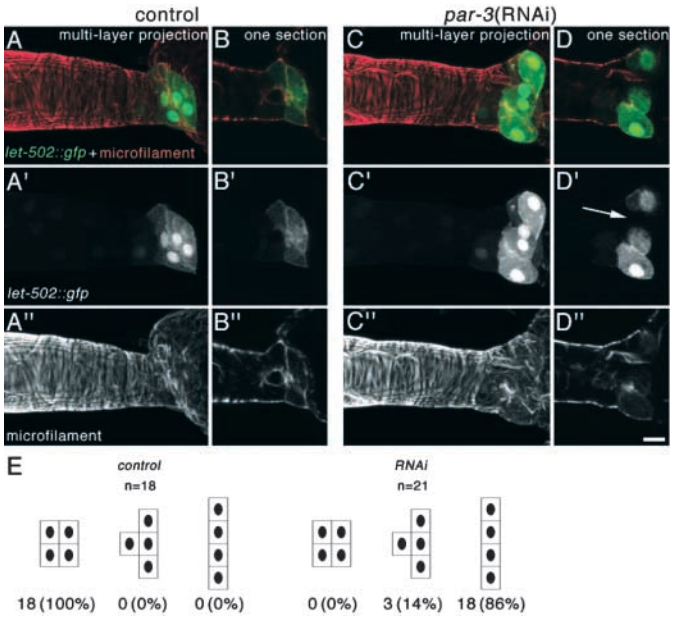

Fig. 4. Specification of spermatheca is not affected by *par-3* RNAi, but distal cell morphology and tissue organization are abnormal. *let-502::gfp* worms were collected after 48 hours of growth with (C,D) or without (A,B) RNAi treatment, and fixed and stained with rhodamine-phalloidin. The number, shape and distribution of cells with high levels of GFP in the distal end of spermatheca was compared. (A,C) Projections of 20 adjacent optical sections. Note the more spherical shape of cells in (C) and the gap between GFP-positive cells in (D′) (arrow). Such gaps are not seen in controls. (E) Summary of the results of the tissue organization analysis. Scale bar: 5 μm.

to failures in ovulation (Clandinin et al., 1998). Specifically, the epidermal growth factor (EGF)-like protein LIN-3, produced in the oocyte, appears to signal through the receptor tyrosine kinase LET-23 in the spermatheca to trigger spermathecal dilation (J. McCarter, M-H. Lee and T. Schedl, personal communication). LET-23 appears to transduce this signal via inositol 1,4,5-triphosphate (IP_3) (Bui and Sternberg, 2002; Clandinin et al., 1998). To test whether defective signaling might contribute to the Emo phenotype of *par-3(RNAi)* worms, we took advantage of the observation that a mutation in *ipp-5*, encoding a putative inositol 5-phosphatase, can suppress mutations in *lin-3* and *let-23* (Bui and Sternberg, 2002). Mutants for *ipp-5* have hyperactive spermathecal dilation, presumably due to aberrant regulation of IP_3-mediated calcium release (Bui and Sternberg, 2002). For the experiment, we grew *ipp-5(sy605)* and *ipp-5*(+) worms from L1 larvae on bacteria producing *par-3* dsRNA or on control bacteria. Using a bacterial culture that produced a strong Emo phenotype in the *ipp-5+;par-3(RNAi)* worms, we found that *ipp-5*;*par-3(RNAi)* worms were nearly as fecund as *ipp-5* worms fed on control bacteria. During a 2.5-hour egg-laying interval *ipp-5;par-3(RNAi)* worms produced an average of 12 eggs per worm (*n*=60 worms), whereas *ipp-5* worms fed on control bacteria produced 15 eggs per worm (*n*=105 worms). As an internal control for the effectiveness of *par-3* RNAi, we scored for maternal effect lethality. Whereas 80% of the eggs laid by *ipp-5* worms fed on control bacteria hatched, only a single worm hatched from eggs laid by *ipp-5;par-3(RNAi)* worms. Thus, *ipp-5(sy605)* partially suppresses the Emo phenotype caused by *par-3(RNAi)*. A sample of 29 *ipp-5;par-3(RNAi)* worms examined under the compound microscope revealed that 18 were completely suppressed, five were Emo in one gonad arm, and six were Emo in both arms. Presumably, these latter two classes of worms account for the reduction in egg production relative to the controls.

The apical organization of distal spermatheca cells is abnormal in *par-3(RNAi)* worms

In order to clarify the basis for the defects in organization and function of the distal spermatheca, we examined the distribution of three proteins with polarized accumulation in epithelial cells: AJM-1, LET-413 and actin.

We first compared the distribution of AJM-1::GFP (Köppen et al., 2001) in control and *par-3(RNAi)* worms grown from L1 at 36, 39 and 42 hours. The adult spermatheca consists of 30 cells that make up an epithelial tube with three distinctive regions (McCarter et al., 1997). Most proximal to the uterus is the spermathecal valve, a specialized multinucleate cell through which embryos must pass to enter the uterus (White, 1988). The middle region consists of 16 cells with circumferential actin cables on the basal surface (Strome, 1986) (Fig. 5E). AJM-1::GFP appears as an irregular and somewhat compressed meshwork that outlines the apical junctions between these cells (Fig. 5A,C). Most distal are a group of four pairs of cells that form a tube with a high concentration of microfilaments adjacent to the lumen; the two most distal cell pairs express high levels of *let-502*::GFP (Wissmann et al., 1999) (Fig. 4A). These distal cells must dilate to allow the mature egg to pass into the spermatheca during ovulation. Just as in the rest of the spermatheca, AJM-1::GFP marks the apical regions of these cells, forming two parallel lines of signal (arrowheads in Fig. 5C). We could detect no discernable and consistent difference between control and *par-3*(RNAi) treated worms in AJM-1::GFP signal in the proximal and middle portions of the spermatheca. However, the distal region of the spermatheca showed consistent disorganization at all three stages examined, as monitored by AJM-1::GFP (*n*>20 in each stage; see Fig. 5B,D). In particular, the two apical lines of AJM-1::GFP were either missing or disrupted and small patches of AJM-1::GFP signal were frequently detected far from the apical region of the cells.

As an additional means of assessing cellular organization, we examined the distribution of LET-413 and actin filaments in the distal spermatheca. *let-413* is the *C. elegans* homolog of *Drosophila melanogaster scribble* that participates in epithelial polarization of embryonic ectoderm (Bilder and Perrimon, 2000; Legouis et al., 2000). LET-413 accumulates along the basolateral surface of epithelial cells including spermathecal cells (Legouis et al., 2000) (Fig. 5A,C,E″,F″). Basolateral restriction of anti-LET-413 antibody or LET-413::GFP was still preserved in the RNAi-treated worms (Fig. 5B,D,E″,F″), although cell shape was consistently aberrant. In control worms, actin forms a cortical meshwork observed just below the basal cell membrane of the spermatheca, with an additional strong accumulation at the apical end in the distal-most cells (*n*=13) (Fig. 5E′, arrows). In *par-3(RNAi)* worms, the apically concentrated actin signal was completely removed (*n*=20) (Fig. 5F′). The observations that both AJM-1 and apical

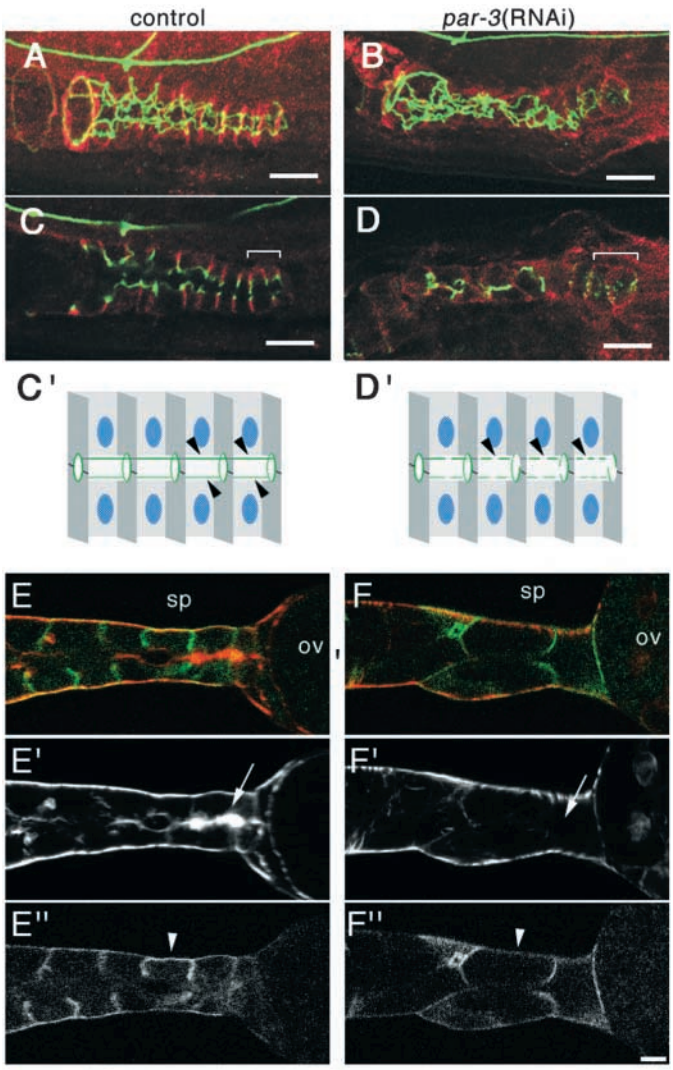

Fig. 5. Apical polarity of spermatheca cells is affected by par-3(RNAi). (A-D) Mislocalization of AJM-1::GFP in spermathecae of RNAi-treated worms. Worms carrying AJM-1::GFP were collected at 39 hours after growth with (right) or without (left) RNAi treatment and localization of AJM-1::GFP and anti-LET-413 was analyzed by confocal microscopy. The distal spermatheca is to the right in all panels; the distal-most cell pairs are indicated by brackets in (C) and (D). Panels (A) and (B) show projections of 36 and 26 optical sections through the entire spermatheca, respectively. (C,D) Single optical sections selected to show the middle focal plane through the distal spermatheca. (C′,D′) Summary of our interpretation of the observed defects in the distal spermatheca. In control worms, AJM-1::GFP is precisely localized to the apical junctions of the distal spermathecal tube (arrowheads). However, in par-3(RNAi) worms, AJM-1::GFP is widely dispersed in puncta that extend into the lateral, and in some worms into the basal, domains. Gaps of GFP signals (arrowheads) are often observed. (E,F) Mislocalization of microfilaments in PAR-3-depleted spermatheca. Worms carrying LET-413::GFP were collected after 48 hours of growth with (right) or without (left) RNAi treatment and stained with rhodamine-phalloidin (red in top panels) after dissection. Ovary (ov) and the spermatheca (sp) are indicated. In control worms, microfilaments are concentrated beneath the apical cell membrane in cells near the distal end of the spermathecal tube (left column, arrow). However, in par-3(RNAi) worms, microfilaments are lacking in this region (right column, arrow). Note that although cell shape is abnormal, LET-413::GFP remains restricted to the basolateral membrane domain (arrowheads). Scale bar: 8 μm (A-D); 5 μm (E-F″).

microfilaments are mislocalized in RNAi-treated worms strongly suggests some aspects of apical-basal polarity are lost in the distal spermathecal cells.

PAR-3, PAR-6 and PKC-3 are transiently expressed and localized asymmetrically in spermathecal precursor cells

To see the correlation between spermathecal defects and the expression pattern of PAR-3, we performed immunohistochemistry with antibody to PAR-3. PAR-3 was detected in the vulval cells, as reported previously (Hurd and Kemphues, 2003) (Fig. 6B′,C′), as well as in most or all somatic gonad precursor cells, including ancestors of uterus, sheath, and spermatheca starting during the third larval stage (L3; about 25-29 hours at 25°C). Figure 6 shows a time-course of the accumulation of PAR-3 and AJM-1 protein during the development of the somatic gonad. PAR-3 began to accumulate in developing uterine, sheath and spermathecal cells during the late-L3 stage. At this stage, PAR-3 appeared to accumulate below the cell membranes that face neighboring cells (Fig. 6A). At this time very little AJM-1 was detected, and what was present was not yet concentrated at apical junctions (compare gonadal cells with vulval cells in Fig. 6A). As development proceeded, asymmetric distribution of PAR-3 became evident (Fig. 6B,C). By the mid-L4 stage most somatic gonad precursors expressed PAR-3, with the exception of cells at the boundary of the uterus and the spermatheca, which we presumed to be precursors of the spemathecal valve (Fig. 6C). Only in mid-L4 did AJM-1 begin to accumulate apically, starting in the proximal gonad and moving more distally (Fig. 6C″,D″). Interestingly, the appearance of AJM-1 at apical junctions roughly correlated with the disappearance of PAR-3 (Fig. 6D).

To determine the effectiveness of the RNAi treatment, we examined the distribution of PAR-3 protein in *par-3(RNAi)* larvae. We carried out these experiments in worms expressing HMP-1::GFP to visualize the cells of the somatic gonad (HMP-1 is the *C. elegans* homolog of α-catenin) (Raich et al., 1999). We saw no clear effect on PAR-3 levels until 27 hours after treatment (not shown). After 30 hours, PAR-3 remained detectable in much of the somatic gonad (Fig. 7B′). However, consistent with the restricted RNAi phenotype, we noted a significant depletion of PAR-3 in the distal-most region of the spermatheca (Fig. 7B′, arrow). By mid-L4 (33 hours), PAR-3 was significantly depleted throughout the gonad (not shown). We also noted that apical accumulation of HMP-1::GFP seemed to proceed from proximal to distal cells (Fig. 7A″ and data not shown) in control animals, and in *par-3(RNAi)* animals HMP::GFP is more extensively disrupted in the distal cells (not shown).

Because PAR-3 co-localizes and acts with PAR-6 and PKC-3 in the early embryo (Hung and Kemphues, 1999; Tabuse et al., 1998) and with PKC-3 and PAR-6 homologs in epithelia in *Drosophila* and mammals (Knust and Bossinger, 2002; Ohno, 2001), we examined the expression of PAR-6 and PKC-

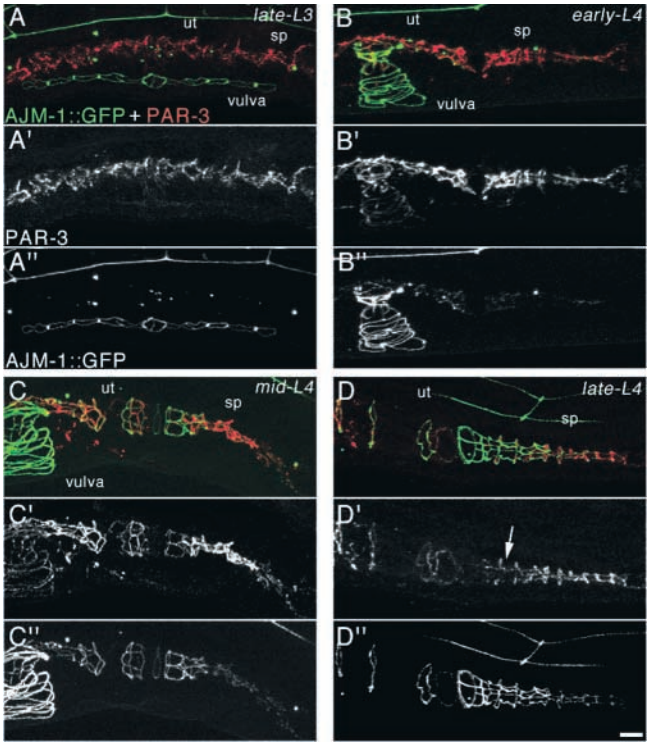

Fig. 6. Time course of PAR-3 and AJM-1::GFP expression. Worms carrying AJM-1::GFP were collected 27 hours (A), 30 hours (B), 33 hours (C), or 36 hours (D) after incubation. Localization of PAR-3 was examined by immunohistochemistry. Multiple sections were stacked in each panel for analysis. PAR-3 was detected in vulval precursor cells (vulva), uterine precursor cells (ut), spermathecal precursor cells (sp) and sheath cells (arrow in B′). PAR-3 levels begin to decrease in 36-hour-incubated worms (arrow in D′). Scale bar: 5 μm.

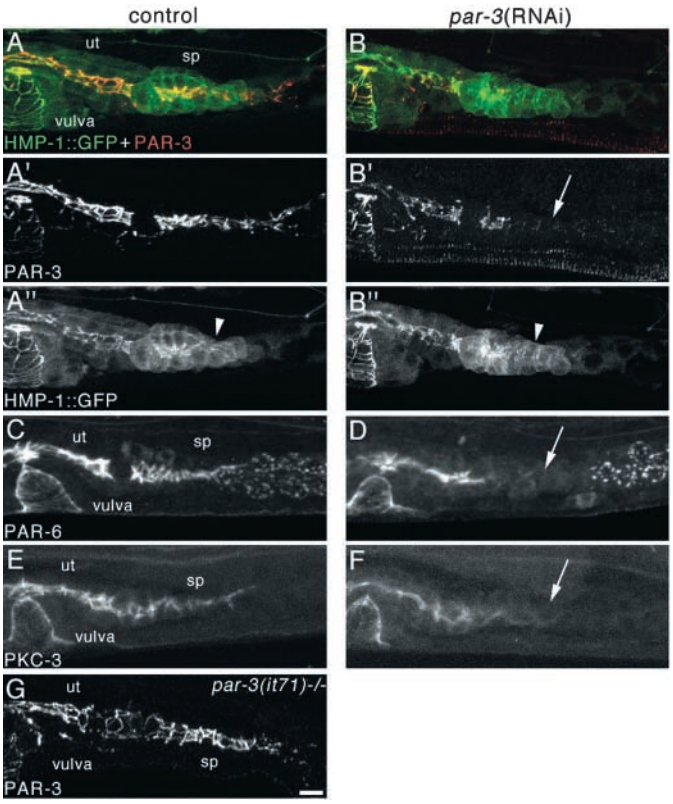

Fig. 7. Effect of par-3 RNAi on expression of PAR-3, PAR-6 and PKC-3. Worms were collected after 30 hours of growth with (right) or without (left) RNAi treatment. Localization of PAR-3 (A,B), PAR-6 (C,D) and PKC-3 (E,F) was examined by immunohistochemistry. Multiple optical sections were stacked in each panel for analysis. The vulval precursor cells (vulva), uterine precursor cells (ut), and spermathecal precursor cells (sp) are indicated. The amounts of all three proteins were significantly reduced in the distal part of the spermathecal primordium (arrows) where cells had not been polarized (arrowheads), as indicated by the absence of apical enrichment of HMP-1::GFP. (L). Expression of PAR-3 in *par-3(it71)* homozygous worms after 30 hours of growth on OP50. Scale bar: 5 μm.

3 in the somatic gonad in control and *par-3(RNAi)* worms. As expected, like PAR-3, both PKC-3 and PAR-6 accumulated at the apical regions of cells in the somatic gonads of worms after 30 hours of growth (n>20 for each) (Fig. 7C,E), and both proteins were selectively lost from the distal spermathecal cells after *par-3* RNAi (Fig. 7D,F).

To determine if this relationship holds true at the functional level, we extended our analysis to examine the effect of *par-6* RNAi and *pkc-3* RNAi on ovulation. For both RNAi experiments, worms grown for 48 hours on RNAi feeding bacteria were stained with DAPI and scored for the Emo phenotype. For *par-6* RNAi, 41/50 worms showed an Emo phenotype; for *pkc-3* RNAi, 17/48 worms showed an Emo phenotype. In the same experiment, 43/47 *par-3(RNAi)* worms and 0/20 control worms were Emo. These findings suggest that PAR-3/PAR-6/PKC-3 act together in the distal spermatheca.

PAR-3 is expressed in somatic gonad precursor cells of *par-3* mutant animals

All existing *par-3* mutations are maternal-effect-lethal mutations; *par-3*–/– progeny of *par-3*+/– mothers grow up to become adults that produce inviable embryos. These worms do not exhibit Emo phenotypes. One of these mutations, *it71*, by genetic and immunological criteria, was judged to be a probable null allele (Cheng et al., 1995; Etemad-Moghadam et al., 1995). Consistent with previous genetic results, we found that the *it71* sequence contained an amber mutation at amino acid position 83. We sequenced a second *par-3* allele, *t1591*, and found that it also contained a nonsense mutation in the extreme amino terminus of the protein (position 38). To address the reason that these alleles do not exhibit an Emo phenotype, we examined PAR-3 accumulation in *par-3(it71)* homozygous larvae. We found that although embryos from *par-3(it71)* mothers fail to accumulate PAR-3 protein (Etemad-Moghadam et al., 1995), the mothers themselves, as larvae, accumulate PAR-3 at normal levels in the developing somatic gonad (n>20) (Fig. 7G). Thus it is possible that all existing *par-3* mutations reside in regions of the protein that are only expressed or required maternally.

Discussion

PAR-3 interacts functionally with PAR-6 and PKC-3 in regulating polarity in early *C. elegans* embryos (Pellettieri and Seydoux, 2002). Studies of homologous molecules isolated

from *Drosophil*a and vertebrates revealed that the proteins interact biochemically and play a widely conserved role in maturation of zonula adherens in polarized epithelial tissues (Knust and Bossinger, 2002; Ohno, 2001). Although polarized distribution of the PAR-3, PAR-6 and PKC-3 proteins has been reported in embryonic gut and epidermal cells in *C. elegans* (Bossinger et al., 2001; McMahon et al., 2001), their role in these tissues has been unclear. We report here the transient expression and asymmetric localization of PAR-3, PAR-6 and PKC-3 during the development of somatic gonad precursor cells in *C. elegan*s. We show that reducing the level of PAR-3, PAR-6 and PKC-3 in this primordium leads to defects in cell polarity in the spermatheca that render it unable to function in ovulation. Thus, the PAR-3/PAR-6/PKC-3 complex is necessary for epithelial polarization in at least one tissue in *C. elegans*. Coupled with recent results uncovering a role for PAR-3 in cell adhesion and gastrulation (Nance et al., 2003), our results indicate that in *C. elegans*, as in other animals, the PAR-3/PAR-6/aPKC complex functions generally to establish polarity in a wide variety of tissues.

PAR-3 is required for spermathecal function

Worms treated with *par-3* RNAi during larval life are sterile and exhibit an Emo phenotype, in which oocytes accumulate in the proximal ovary with endomitotic nuclei. We determined, using *rrf-1*, a mutant in which RNAi is blocked in the soma but not the germline (Sijen et al., 2001), that the Emo phenotype resulted mainly, perhaps entirely, from a defect in the soma, most likely a defect in ovulation. Direct observations of defective first ovulations in *par-3(RNAi)* worms confirmed this.

Successful ovulation requires contractions of the sheath cells in the proximal gonad in conjunction with dilation of the distal spermatheca (McCarter et al., 1997; Rose et al., 1997). Three observations suggest that the basis for defective ovulation after *par-3* RNAi is a failure in spermathecal function. First, sheath cells undergo extensive contraction, are organized normally and express appropriate differentiation markers. Second, in spite of extensive sheath cell contractions, the spermatheca fails to dilate to cover the mature eggs. Third, sperm accumulate exclusively in the proximal gonad and are not detected in the spermathecae of affected worms.

Our microscopic examination of spermathecae revealed clear morphological abnormalities in the four distal-most cells. These cells pair to form a narrow tube in control animals. However, in *par-3(RNAi)* worms, the distal cells are more randomly positioned with respect to each other and fail to form the tight arrangement observed in the wild type. This raised the possibility that the spermatheca was physically blocked, preventing passage of eggs. However, as described below, we found that this was not the case in most Emo worms.

PAR-3 depletion results in defective oocyte/spermatheca signaling

In normal worms, dilation of the spermatheca requires signaling from the oocyte to the spermatheca that depends upon the epidermal-growth-factor type ligand LIN-3 and the receptor tyrosine kinase LET-23 and upon components of the inositol phosphate signaling system (Bui and Sternberg, 2002; Clandinin et al., 1998). Reduction-of-function mutations in *let-23* and *lin-3* that cause Emo phenotypes can be suppressed by loss-of-function mutations in *ipp-5*, a gene encoding a type I 5-phosphatase. Like other 5-phosphatases (Majerus, 1992), IPP-5 presumably negatively regulates inositol signaling by dephosphorylating 1,4,5 inositol triphosphate (Bui and Sternberg, 2002). We found that the *ipp-5* mutation effectively suppressed the effects of PAR-3 depletion, arguing strongly that the Emo phenotype results from a defect in signaling between the oocyte and the spermatheca. The incomplete suppression of the Emo phenotype in *par-3(RNAi)* worms, in contrast to the strong suppression of *let-23* and *lin-3* mutants (Bui and Sternberg, 2002), however, raises the possibility that some *par-3(RNAi)* worms might have structural defects that cannot be suppressed by *ipp-5*.

Apical organization of the distal spermathecal cells require PAR-3

We propose that the primary defect caused by *par-3* RNAi is in the organization of the apical domain of the distal spermathecal cells. Although we cannot rule out a subtle defect in cell fate specification or in the asymmetric divisions leading to the formation of the spermatheca, *par-3* RNAi has no detectable effect on cell numbers or on the expression of cell fate markers. We observed that PAR-3 starts to accumulate in the late-L3 stage and localizes to the apical regions prior to AJM-1, a marker for apical organization. This suggests that PAR-3 could play a role early in the polarization of this tissue. In fact, this idea is supported by our finding that removal of PAR-3 from precursors in the distal half of the spermatheca resulted in mislocalization of AJM-1 and apical microfilaments in these cells. Suppression by *ipp-5* argues that a consequence of apical disorganization is a mislocalization of the signal transduction machinery in the distal spermathecal cells.

The effect of PAR-3 depletion on oocyte/spermathecal signaling is strikingly reminiscent of the effect of mutations in *lin-2*, *lin-7* and *lin-10* on LIN-3/LET-23 signaling during vulval development (Kaech et al., 1998). In the vulva, LIN-2, LIN-7 and LIN-10 proteins act in a complex to ensure the basolateral accumulation of LET-23; inactivation of the complex results in failure of vulval induction (Kaech et al., 1998). Unfortunately, we were unable to detect LET-23 protein in the distal spermatheca to assess whether LET-23 distribution was affected by depletion of PAR-3.

A restricted role for PAR-3 in the distal spermatheca?

It is puzzling that in spite of widespread expression of PAR-3 in the somatic gonad, defects are only observable at the extreme distal end of the spermatheca. Although this could reflect the only requirement for PAR-3 in post-embryonic development, it is also possible that *par-3* RNAi is ineffective in revealing a more general post-embryonic requirement for PAR-3. We propose that the more restricted *par-3(RNAi)* phenotype arises as a combination of incomplete depletion of the protein at early stages of gonadal development, the relatively late development of the distal spermatheca and the absence of a role for PAR-3 in maintenance of the apical organization. Gonadal development proceeds from proximal to distal tissues, with proximal cells undergoing terminal differentiation while the distal cells are still proliferating (Kimble and Hirsh, 1979). In particular, we note that α-catenin and AJM-1 are recruited into apical junctions in a proximal-

distal direction (see Fig. 6C″,D″ and Fig. 7A″). Inversely correlating with this difference, after RNAi, PAR-3 is first depleted from the distal spermathecal cells, perhaps because the newly formed apical junctions in the proximal cells block the rapid turnover of the protein. By the time that the bulk of the PAR-3 protein has been depleted from the more proximal gonad, PAR-3 might no longer be required. This possibility is suggested by observations that dominant negative mutations in aPKC and PAR-6 affect establishment but not maintenance of polarity in MDCK cells (Suzuki et al., 2001; Yamanaka et al., 2001).

An unexpected result of our analysis is the existence of PAR-3 proteins in homozygous *par-3(it71)* larvae. This allele has a nonsense mutation at the 83rd codon. Our antibody was raised against the central domain of PAR-3, and no protein is detected in embryos produced by homozygous worms (Etemad-Moghadam et al., 1995). There are two possible explanations for the source of the larval signal in the mutant homozygotes. One possibility is that the maternal supply of wild-type mRNA is sufficient for both embryonic and post-embryonic development. This seems unlikely, because the entire somatic gonad (143 cells) arises from only two blast cells (out of the 558 embryonic cells), and considerable dilution of the maternal products must take place. The other possibility is that post-embryonic PAR-3 protein is translated from an mRNA that differs from the embryonic message and is unaffected by any existing mutation. This is quite possible, since the screens to identify most existing mutations were maternal-effect-lethal screens that would not have detected zygotic lethal or sterile mutations. Unfortunately, no complete *par-3* cDNAs are present in available databases, and our attempts to identify a post-embryonic-specific mRNA or protein isoform have not yet been successful.

From extensive studies, PAR-3 is known to interact with PAR-6 and PKC-3 during cell polarization in various systems. Here we report observations providing evidence that PAR-3, PAR-6 and PKC-3 also work together in organizing apical domains during somatic gonad development in *C. elegans*. The three proteins show similar distributions in the developing somatic gonad, and distributions of PKC-3 and PAR-6 are dependent upon PAR-3, as shown by *par-3* RNAi. Furthermore, removal of PAR-6 and PKC-3 by RNAi produces a phenotype similar to that of *par-3* RNAi. It is possible that the complex functions in the same way in *C. elegans* as it does in other systems. At least one aspect of the relationship between the PAR-3(Bazooka)/PAR-6/PKC-3 complex and LET-413(Scribble) appears to be conserved in flies and worms. In the embryonic ectoderm of flies, the Bazooka/PAR-6/aPKC domain expands in the absence of Scribble, whereas Scribble distribution is insensitive to removal of Bazooka (Bilder et al., 2003; Tanentzapf and Tepass, 2003). Similarly, we found that the distribution of LET-413 was normal in distal spermathecal cells after the removal of PAR-3 (Fig. 5B,D,E,F), and in studies in the intestinal epithelium the apical domain of the PAR-3/PAR-6/PKC-3 complex was shown to expand after removal of LET-413 (McMahon et al., 2001).

In summary, PAR-3 accumulates apically in somatic gonad precursor cells. PAR-3 activity is required in the distal spermatheca for the proper localization of AJM-1::GFP, an apical marker, and microfilaments. The loss of polarity in the distal spermatheca correlates with defective ovulation (Emo phenotype) and mislocalization of mature sperm in the adult. We propose that loss of epithelial polarity in the spermathecal cells results in failure to organize the cortical signal transduction system required for spermathecal dilation and might in extreme cases lead to blockage of the spermathecal lumen. Based on these findings, we propose that spermathecal development in *C. elegans* has the potential to serve as a model system to address the question of how cells acquire asymmetric properties and, in particular, how cells interact to form epithelial tubes.

We thank Daryl Hurd for sharing the intitial observation that *par-3* RNAi results in sterility and for providing constructs for *par-6* RNAi and *pkc-3* RNAi. We thank Jeff Hardin, Paul Mains, David Greenstein, Ralf Schnabel, David Miller and Paul Sternberg for strains and antibodies. Some strains were obtained from the *Caenorhabditis* Genetics Center, which is funded by the NIH Center for Research Resources. We also thank Tim Schedl for the suggestion to use *rrf-1* to test the somatic requirement for PAR-3, and Katherine Baker and Mona Hassab for technical support. This work was supported by a Long-Term Fellowship from the Human Frontiers Science Program to S.A. and by grant R01 HD27689 from the National Institutes of Child Health and Development to K.J.K.

References

Betschinger, J., Mechtler, K. and Knoblich, J. A. (2003). The Par complex directs asymmetric cell division by phosphorylating the cytoskeletal protein Lgl. *Nature* **422**, 326-330.

Bilder, D. and Perrimon, N. (2000). Localization of apical epithelial determinants by the basolateral PDZ protein Scribble. *Nature* **403**, 676-680.

Bilder, D., Schober, M. and Perrimon, N. (2003). Integrated activity of PDZ protein complexes regulates epithelial polarity. *Nat. Cell Biol.* **5**, 53-58.

Bossinger, O., Klebes, A., Segbert, C., Theres, C. and Knust, E. (2001). Zonula adherens formation in Caenorhabditis elegans requires dlg-1, the homologue of the Drosophila gene discs large. *Dev. Biol.* **230**, 29-42.

Bui, Y. K. and Sternberg, P. W. (2002). Caenorhabditis elegans inositol 5-phosphatase homolog negatively regulates inositol 1,4,5-triphosphate signaling in ovulation. *Mol. Biol. Cell* **13**, 1641-1651.

Cheng, N. N., Kirby, C. M. and Kemphues, K. J. (1995). Control of cleavage spindle orientation in Caenorhabditis elegans, the role of the genes par-2 and par-3. *Genetics* **139**, 549-559.

Clandinin, T. R., DeModena, J. A. and Sternberg, P. W. (1998). Inositol trisphosphate mediates a RAS-independent response to LET-23 receptor tyrosine kinase activation in C. elegans. *Cell* **92**, 523-533.

Etemad-Moghadam, B., Guo, S. and Kemphues, K. J. (1995). Asymmetrically distributed PAR-3 protein contributes to cell polarity and spindle alignment in early C. elegans embryos. *Cell* **83**, 743-752.

Greenstein, D., Hird, S., Plasterk, R. H., Andachi, Y., Kohara, Y., Wang, B., Finney, M. and Ruvkun, G. (1994). Targeted mutations in the Caenorhabditis elegans POU homeo box gene ceh-18 cause defects in oocyte cell cycle arrest, gonad migration, and epidermal differentiation. *Genes Dev.* **8**, 1935-1948.

Hung, T. J. and Kemphues, K. J. (1999). PAR-6 is a conserved PDZ domain-containing protein that colocalizes with PAR-3 in Caenorhabditis elegans embryos. *Development* **126**, 127-135.

Hurd, D. D. and Kemphues, K. J. (2003). PAR-1 is required for morphogenesis of the Caenorhabditis elegans vulva. *Dev. Biol.* **253**, 54-65.

Hurd, T. W., Gao, L., Roh, M. H., Macara, I. G. and Margolis, B. (2003). Direct interaction of two polarity complexes implicated in epithelial tight junction assembly. *Nat. Cell Biol.* **5**, 137-142.

Iwasaki, K., McCarter, J., Francis, R. and Schedl, T. (1996). emo-1, a Caenorhabditis elegans Sec61p gamma homologue, is required for oocyte development and ovulation. *J. Cell Biol.* **134**, 699-714.

Izumi, Y., Hirose, T., Tamai, Y., Hirai, S., Nagashima, Y., Fujimoto, T., Tabuse, Y., Kemphues, K. J. and Ohno, S. (1998). An atypical PKC directly associates and colocalizes at the epithelial tight junction with ASIP, a mammalian homologue of Caenorhabditis elegans polarity protein PAR-3. *J. Cell Biol.* **143**, 95-106.

Johnson, K. and Wodarz, A. (2003). A genetic hierarchy controlling cell polarity. *Nat. Cell Biol.* **5**, 12-14.

Kaech, S. M., Whitfield, C. W. and Kim, S. K. (1998). The LIN-2/LIN-7/LIN-10 complex mediates basolateral membrane localization of the C. elegans EGF receptor LET-23 in vulval epithelial cells. *Cell* **94**, 761-771.

Kemphues, K. J. and Strome, S. (1997). Fertilization and establishment of polarity in the embryo. In *C. elegans II* (ed. D. L. Riddle, T. Blumenthal, B. J. Meyer and J. R. Priess), pp. 335-359. Cold Spring Harbor, NY: Cold Spring Harbor Laboratory Press.

Kimble, J. and Hirsh, D. (1979). The postembryonic cell lineages of the hermaphrodite and male gonads in Caenorhabditis elegans. *Dev. Biol.* **70**, 396-417.

Knust, E. and Bossinger, O. (2002). Composition and formation of intercellular junctions in epithelial cells. *Science* **298**, 1955-1959.

Köppen, M., Simske, J. S., Sims, P. A., Firestein, B. L., Hall, D. H., Radice, A. D., Rongo, C. and Hardin, J. D. (2001). Cooperative regulation of AJM-1 controls junctional integrity in Caenorhabditis elegans epithelia. *Nat. Cell Biol.* **3**, 983-991.

Kuchinke, U., Grawe, F. and Knust, E. (1998). Control of spindle orientation in Drosophila by the Par-3-related PDZ-domain protein Bazooka. *Curr. Biol.* **8**, 1357-1365.

Legouis, R., Gansmuller, A., Sookhareea, S., Bosher, J. M., Baillie, D. L. and Labouesse, M. (2000). LET-413 is a basolateral protein required for the assembly of adherens junctions in Caenorhabditis elegans. *Nat. Cell Biol.* **2**, 415-422.

Leung, B., Hermann, G. J. and Priess, J. R. (1999). Organogenesis of the Caenorhabditis elegans intestine. *Dev. Biol.* **216**, 114-134.

Lewis, J. A. and Fleming, J. T. (1995). Basic culture methods. In *Methods in Cell Biology*. Vol. 48 (ed. H. F. Epstein and D. C. Shakes), pp. 3-29. San Diego: Academic Press.

Majerus, P. W. (1992). Inositol phosphate biochemistry. *Annu. Rev. Biochem.* **61**, 225-250.

McCarter, J., Bartlett, B., Dang, T. and Schedl, T. (1997). Soma-germ cell interactions in Caenorhabditis elegans, multiple events of hermaphrodite germline development require the somatic sheath and spermathecal lineages. *Dev. Biol.* **181**, 121-143.

McCarter, J., Bartlett, B., Dang, T. and Schedl, T. (1999). On the control of oocyte meiotic maturation and ovulation in Caenorhabditis elegans. *Dev. Biol.* **205**, 111-128.

McMahon, L., Legouis, R., Vonesch, J. L. and Labouesse, M. (2001). Assembly of C. elegans apical junctions involves positioning and compaction by LET-413 and protein aggregation by the MAGUK protein DLG-1. *J. Cell Sci.* **114**, 415-422.

Michaux, G., Legouis, R. and Labouesse, M. (2001). Epithelial biology, lessons from Caenorhabditis elegans. *Gene* **277**, 83-100.

Miller, D. M. and Shakes, D. C. (1995). Immunofluorescence microscopy. In *Caenorhabditis elegans: Modern Biological Analysis of an Organism*. Vol. 48 (ed. H. F. Epstein and D. C. Shakes), pp. 365-394. San Diego: Academic Press.

Miller, D. M., Stockdale, F. E. and Karn, J. (1986). Immunological identification of the genes encoding the four myosin heavy chain isoforms of Caenorhabditis elegans. *Proc. Natl. Acad. Sci. USA* **83**, 2305-2309.

Miller, M. A., Nguyen, V. Q., Lee, M. H., Kosinski, M., Schedl, T., Caprioli, R. M. and Greenstein, D. (2001). A sperm cytoskeletal protein that signals oocyte meiotic maturation and ovulation. *Science* **291**, 2144-2147.

Miller, M. A., Ruest, P. J., Kosinski, M., Hanks, S. K. and Greenstein, D. (2003). An Eph receptor sperm-sensing control mechanism for oocyte meiotic maturation in Caenorhabditis elegans. *Genes Dev.* **17**, 187-200.

Mohler, W. A., Simske, J. S., Williams-Masson, E. M., Hardin, J. D. and White, J. G. (1998). Dynamics and ultrastructure of developmental cell fusions in the Caenorhabditis elegans hypodermis. *Curr. Biol.* **8**, 1087-1090.

Nance, J., Munro, E. M. and Priess, J. R. (2003). C. elegans PAR-3 and PAR-6 are required for apicobasal asymmetries associated with cell adhesion and gastrulation. *Development* **130**, 5339-5350.

Ohno, S. (2001). Intercellular junctions and cellular polarity, the PAR-aPKC complex, a conserved core cassette playing fundamental roles in cell polarity. *Curr. Opin. Cell Biol.* **13**, 641-648.

Pellettieri, J. and Seydoux, G. (2002). Anterior-posterior polarity in C. elegans and Drosophila–PARallels and differences. *Science* **298**, 1946-1950.

Plant, P. J., Fawcett, J. P., Lin, D. C., Holdorf, A. D., Binns, K., Kulkarni, S. and Pawson, T. (2003). A polarity complex of mPar-6 and atypical PKC binds, phosphorylates and regulates mammalian Lgl. *Nat. Cell Biol.* **5**, 301-308.

Raich, W. B., Agbunag, C. and Hardin, J. (1999). Rapid epithelial-sheet sealing in the Caenorhabditis elegans embryo requires cadherin-dependent filopodial priming. *Curr. Biol.* **9**, 1139-1146.

Rose, K. L., Winfrey, V. P., Hoffman, L. H., Hall, D. H., Furuta, T. and Greenstein, D. (1997). The POU gene ceh-18 promotes gonadal sheath cell differentiation and function required for meiotic maturation and ovulation in Caenorhabditis elegans. *Dev. Biol.* **192**, 59-77.

Sijen, T., Fleenor, J., Simmer, F., Thijssen, K. L., Parrish, S., Timmons, L., Plasterk, R. H. and Fire, A. (2001). On the role of RNA amplification in dsRNA-triggered gene silencing. *Cell* **107**, 465-476.

Strome, S. (1986). Fluorescence visualization of the distribution of microfilaments in gonads and early embryos of the nematode Caenorhabditis elegans. *J. Cell Biol.* **103**, 2241-2252.

Suzuki, A., Yamanaka, T., Hirose, T., Manabe, N., Mizuno, K., Shimizu, M., Akimoto, K., Izumi, Y., Ohnishi, T. and Ohno, S. (2001). Atypical protein kinase C is involved in the evolutionarily conserved par protein complex and plays a critical role in establishing epithelia-specific junctional structures. *J. Cell Biol.* **152**, 1183-1196.

Tabuse, Y., Izumi, Y., Piano, F., Kemphues, K. J., Miwa, J. and Ohno, S. (1998). Atypical protein kinase C cooperates with PAR-3 to establish embryonic polarity in Caenorhabditis elegans. *Development* **125**, 3607-3614.

Tanentzapf, G. and Tepass, U. (2003). Interactions between the crumbs, lethal giant larvae and bazooka pathways in epithelial polarization. *Nat. Cell Biol.* **5**, 46-52.

Timmons, L., Court, D. L. and Fire, A. (2001). Ingestion of bacterially expressed dsRNAs can produce specific and potent genetic interference in Caenorhabditis elegans. *Gene* **263**, 103-112.

Ward, S. and Carrel, J. S. (1979). Fertilization and sperm competition in the nematode Caenorhabditis elegans. *Dev. Biol.* **73**, 304-321.

Watts, J. L., Etemad-Moghadam, B., Guo, S., Boyd, L., Draper, B. W., Mello, C. C., Priess, J. R. and Kemphues, K. J. (1996). par-6, a gene involved in the establishment of asymmetry in early C. elegans embryos, mediates the asymmetric localization of PAR-3. *Development* **122**, 3133-3140.

White, J. (1988). The anatomy. In *The Nematode Caenorhabditis elegans* (ed. W. B. Wood), pp. 81-122. Cold Spring Harbor, NY: Cold Spring Harbor Laboratory Press.

Wissmann, A., Ingles, J. and Mains, P. E. (1999). The Caenorhabditis elegans mel-11 myosin phosphatase regulatory subunit affects tissue contraction in the somatic gonad and the embryonic epidermis and genetically interacts with the Rac signaling pathway. *Dev. Biol.* **209**, 111-127.

Yamanaka, T., Horikoshi, Y., Sugiyama, Y., Ishiyama, C., Suzuki, A., Hirose, T., Iwamatsu, A., Shinohara, A. and Ohno, S. (2003). Mammalian Lgl forms a protein complex with PAR-6 and aPKC independently of PAR-3 to regulate epithelial cell polarity. *Curr. Biol.* **13**, 734-743.

Yamanaka, T., Horikoshi, Y., Suzuki, A., Sugiyama, Y., Kitamura, K., Maniwa, R., Nagai, Y., Yamashita, A., Hirose, T., Ishikawa, H. et al. (2001). PAR-6 regulates aPKC activity in a novel way and mediates cell-cell contact-induced formation of the epithelial junctional complex. *Genes Cells* **6**, 721-731.